

# Lipopolysaccharide (LPS) extracted from *Bacteroides vulgatus* effectively prevents LPS extracted from *Escherichia coli* from inducing epithelial-mesenchymal transition

YUPING LI<sup>1</sup>, MENG DAN XU<sup>2</sup>, HAIYING ZHAI<sup>3</sup>, CHANGFU YANG<sup>1</sup>, JIAOTONG YANG<sup>1</sup>, ZUNLI KE<sup>1</sup>, WANHAO CHEN<sup>1</sup>, JIANGQIN OU<sup>3</sup>, ZONGGE SHA<sup>1</sup> and QIAOQIAO XIAO<sup>1</sup>

<sup>1</sup>Basic Medical School, Guizhou University of Traditional Chinese Medicine, Guiyang, Guizhou 550025;

<sup>2</sup>Shizhen College, Guizhou University of Traditional Chinese Medicine, Guiyang, Guizhou 550200;

<sup>3</sup>The First Affiliated Hospital, Guizhou University of Traditional Chinese Medicine, Guiyang, Guizhou 550000, P.R. China

Received March 15, 2023; Accepted August 9, 2023

DOI: 10.3892/mmr.2023.13082

**Abstract.** Pathological epithelial-mesenchymal transition (EMT) has been shown to fulfill a key role in the development and progression of a variety of lung diseases. It has been demonstrated that the inflammatory microenvironment is a decisive factor in inducing pathological EMT. Hexacylated lipopolysaccharide (LPS) [or proacylated lipopolysaccharide (P-LPS), which functions as proinflammatory lipopolysaccharide] is one of the most effective Toll-like receptor 4 (TLR4) agonists. Furthermore, the pentacylated and tetracylated form of lipopolysaccharide (or A-LPS, which functions as anti-inflammatory lipopolysaccharide) has been shown to elicit competitive antagonistic effects against the pro-inflammatory activity of P-LPS. At present, it remains unclear whether LPS extracted from *Bacteroides vulgatus* (BV-LPS) can prevent LPS extracted from *Escherichia coli* (EC-LPS) from inducing pathological EMT. In the present study, A549 cells and C57BL/6 mice lung tissue were both induced by EC-LPS (P-LPS) and BV-LPS (A-LPS), either alone or in combination. The anticipated anti-inflammatory effects of BV-LPS were analyzed by examining the lung coefficient, lung pathology, A549 cell morphology and expression levels both of the inflammatory cytokines, IL-1 $\beta$ , IL-6 and TNF- $\alpha$  and of the EMT signature proteins, epithelial cadherin (E-cadherin),  $\alpha$ -smooth muscle actin ( $\alpha$ -SMA) and vimentin.

In addition, the expression levels of TLR4, bone morphogenic protein and activin membrane-bound inhibitor (BAMBI) and Snail were detected and the possible mechanism underlying how BV-LPS may prevent EC-LPS-induced EMT was analyzed. The results obtained showed that the morphology of the A549 cells was significantly polarized, the lung index was significantly increased, the alveolar structure was collapsed and the expression levels of IL-1 $\beta$ , IL-6, TNF- $\alpha$ ,  $\alpha$ -SMA, vimentin, TLR4 and Snail in both lung tissue and A549 cells were significantly increased, whereas those of E-cadherin and BAMBI were significantly decreased. Treatment with BV-LPS in combination with EC-LPS was found to reverse these changes. In conclusion, the present study demonstrated that BV-LPS is able to effectively prevent EC-LPS-induced EMT in A549 cells and in mouse lung tissue and furthermore, the underlying mechanism may be associated with inhibition of the TLR4/BAMBI/Snail signaling pathway.

## Introduction

Epithelial-mesenchymal transition (EMT) is an important process of embryonic development and a normal physiological phenomenon associated with tissue repair (1). However, pathological EMT has been shown to exert a key role in the occurrence and development of numerous lung diseases, including asthma, acute respiratory distress syndrome and chronic obstructive pulmonary disease (2-4).

It has previously been demonstrated that the inflammatory microenvironment is a decisive factor in inducing pathological EMT (5). The activity of lipopolysaccharide (LPS) is significantly affected by changes in sugar composition, the length and arrangement (as well as the modification) of the lipid A, core oligosaccharides and the glycochain structure of O antigen (6), among which the number of lipid A acyl chains present is an important determinant of immune activation (7). A previous study showed that hexacylated (proacylated) LPS (P-LPS) was one of the most effective Toll-like receptor 4 (TLR4) agonists. By contrast, the pentacylated and tetracylated lipopolysaccharide (A-LPS) exerted a competitive antagonistic effect on the pro-inflammatory activity of P-LPS (8).

---

*Correspondence to:* Dr Haiying Zhai, The First Affiliated Hospital, Guizhou University of Traditional Chinese Medicine, 71 Baoshan North Road, Guiyang, Guizhou 550000, P.R. China  
E-mail: zhhy1005@gzy.edu.cn

Professor Changfu Yang, Basic Medical School, Guizhou University of Traditional Chinese Medicine, 4 Dongqingnan Road, Guiyang, Guizhou 550025, P.R. China  
E-mail: yangchangfu@126.com

**Key words:** *Bacteroides vulgatus*, inflammation, proinflammatory lipopolysaccharide, anti-inflammatory lipopolysaccharide, epithelial-mesenchymal transition

Intestinal flora fulfill a crucial role in maintaining host intestinal homeostasis. Under normal circumstances, host intestinal inflammation does not occur, which is due to the optimal control of P-LPS activity via the dynamic balance of various intestinal flora, which enable the host to maintain intestinal homeostasis. Among the human intestinal flora, the phylum Proteobacteria is a major contributor to P-LPS synthesis, whereas the phylum Bacteroidetes is a major contributor to A-LPS synthesis, producing A-LPS that antagonizes the pro-inflammatory activity of P-LPS, thereby driving the process of immunosilencing throughout the intestinal environment. In the case of colitis regulated by A-LPS, mice with low abundance of Proteobacteria and high abundance of Bacteroidetes show low levels of intestinal endotoxin and maintained mucosal immune homeostasis (9). Conversely, mice with high abundance of Proteobacteria and low abundance of Bacteroidetes are more likely to develop colitis (9). Similar to the situation in the gut, LPS in the lung is mainly derived from the intestinal flora and TLR4 is widely distributed in lung tissue (10,11).

However, to the best of the authors' knowledge, whether A-LPS can effectively prevent P-LPS-induced pulmonary inflammation and pathological EMT has yet to be reported. Therefore, in the present study, lung epithelial cells and mouse lung tissues were induced by A-LPS and P-LPS either alone or in combination to explore whether A-LPS is able to effectively prevent the P-LPS-induced inflammatory response and pathological EMT.

## Material and methods

**Bacterial strains and LPS.** For the present study, *B. vulgatus* was purchased from the China Typical Culture Preservation Center (strain preservation number: CCTCC AB 2015378). BV-LPS purification was performed according to the hot phenol-water method (12), whereas EC-LPS extracted from the membrane of *E. coli* 055:B5 was purchased from MilliporeSigma.

**Cell culture and viability examination.** Human type II alveolar epithelial A549 cells were purchased from the Type Culture Collection of the Chinese Academy of Sciences and cultured in DMEM medium supplemented with 10% fetal bovine serum (cat. no. S9030; Beijing Solarbio Technology Co., Ltd.), 100 U/ml penicillin and 100 ng/ml streptomycin at 37°C in a humidified atmosphere comprising 5% CO<sub>2</sub>/95% air. Cell viability was assessed using the 3-(4,5-dimethylthiazol-2-yl)-2,5-diphenyltetrazolium bromide (MTT) assay (cat. no. M6494; Thermo Fisher Scientific, Inc.). After seeding the A549 cells (2x10<sup>4</sup> cells/ml) into the wells of a 96-well plate, the cells were treated with BV-LPS (0, 2.5, 5, 10, 20, 40, 80, 160 or 320 µg/ml) or EC-LPS (0, 1, 2, 5, 10, 15 or 20 µg/ml) for 72 h. After 72 h, the medium was removed and the cells were washed three times with phosphate-buffered saline (PBS). Subsequently, 20 µl MTT (final concentration, 5 mg/ml) was added to each well and the plates were incubated at 37°C for 4 h. The MTT solution was then removed and 100 µl dimethyl sulfoxide was added to dissolve the colored formazan crystals. Finally, the optical density was measured at a wavelength of 490 nm using a microplate reader (Thermo Fisher Scientific, Inc.) and cell viability was calculated as the percentage of the absorbance of untreated control cells.

**Induction of A549 cells by drug administration.** The cells were divided into the following four experimental groups: Control group (Control), EC-LPS group (EC), BV-LPS group (BV) and combined group (EC-BV). To observe the effect of BV-LPS on the prevention of EMT induced by EC-LPS in A549 cells, after the cells had reached 80% confluence they were treated with EC-LPS (10 µg/ml) and BV-LPS (60 µg/ml) (13,14) either alone or in combination for up to 48 h. The morphological changes of cells were subsequently observed and recorded using an inverted phase contrast microscope (DP73; Olympus Corporation). The extent of inflammation and EMT were then detected by reverse transcription-quantitative (RT-q)PCR, immunofluorescence staining and western blotting analyses, as detailed below.

**Animal feeding and experimental protocols.** A total of 40 nine-week old male C57BL/6 mice (18-20 g) were obtained from the Institute of Laboratory Animals, Guizhou University of Traditional Chinese Medicine. The mice were housed under conditions of a 12-h light/dark cycle with free access to tap water and standard chow (cat. no. D12450B; Research Diets, Inc.) at a temperature of 22±1°C and a relative humidity of 50-70% and received one daily health observation. The present study was approved by the Experimental Animal Ethics Committee of Guizhou University of Traditional Chinese Medicine (approval number: 20220039).

**Induction of mouse lung tissue by drug administration.** The mice were randomly divided into the Control, EC, BV and EC-BV groups as mentioned above, with 10 mice in each group. To observe the effect of BV-LPS on preventing EMT induced by EC-LPS in lung tissue of mice, after following a protocol of adaptive feeding for 1 week, the mice were anesthetized with 1% (v/v) sodium pentobarbital injected intraperitoneally (40 mg/kg) and the mice were subsequently administered EC-LPS (5 mg/kg) and BV-LPS (30 mg/kg) (13,15) either alone or in combination, with pulmonary administration via airway intubation (administration volume; 2.5 ml/kg) (16,17). After 28 days of normal feeding, none of the mice in the study reached the humane endpoints (including labored breathing, nasal discharge, lethargy or persistent recumbency, difficulty with ambulation or an inability to obtain food or water). Mice were anesthetized with 20% urethane injected intraperitoneally (2,000 mg/kg) prior to sacrifice of the mice by cervical dislocation of the spine. Subsequently, the mice were weighed, dissected and the lung tissue was collected for weighing. The left-lobe lung was then fixed in 4% paraformaldehyde solution (Beijing Solarbio Technology Co., Ltd.) at room temperature for 48 h, whereas the right-lobe lung was directly frozen in liquid nitrogen and later transferred to the refrigerator at -80°C for storage. The percentages of lung mass/body mass were used for the lung index.

**Cell morphological observation.** To obtain the morphological images, A549 cells were visualized and images captured using a phase-contrast microscope equipped with a digital camera (Leica DM IL; Leica Microsystems GmbH).

**Immunofluorescence staining.** A549 cells were seeded into 24-well plates with adhesive slides at the density of 1x10<sup>3</sup> cells/ml and the cells were divided into the Control, EC, BV and EC-BV

Table I. Primer sequences used in the present study.

Gene name	Forward, 5'→3'	Reverse, 5'→3'
IL-1 $\beta$ (h)	ACGATGCACCTGTACGATCA	TCTTTCAACACGCAGGACAG
IL-6 (h)	GATGAGTACAAAAGTCCTGATCCA	CTGCAGCCACTGGTTCTGT
TNF- $\alpha$ (h)	CTCCTCACCCACACCATCAGCCGCA	ATAGATGGGCTCATACCAGGGCTTG
GAPDH (h)	AACAGCGACACCCACTCCTC	GGAGGGGAGATTCAAGTGTG
IL-1 $\beta$ (m)	CAAGGAGAACCAAGCAACGA	TTTCATTACACAGGACAGGTATAGA
IL-6 (m)	ACTTCCATCCAGTTGCCTTCTTGG	TAAAGCCTCCGATTGTGAAGTG
TNF- $\alpha$ (m)	AGGTTCTCTTCAAGGGACAA	GACTTTCTCCTGGTATGAGATAG
TLR4 (m)	CGCTTTCACCTCTGCCTTCAC	TTGCCGTTTCTTGTCTTCTTC
BAMBI (m)	CTCAAATTCCTCCACTCACCCA	GCTGATACCTGTTTCCTTGTCTCG
Snail (m)	TTTACCTTCCAGCAGCCCTA	CCCCTGTCTCATCTGACA
GAPDH (m)	CCTCGTCCCGTAGACAAAATG	TCTCCACTTTGCCACTGCAA

h, human primer; m, mouse primer; TLR4, Toll-like receptor 4; BAMBI, bone morphogenic protein and activin membrane-bound inhibitor.

groups, with 3 wells in each group. After the A549 cells had been attached to the plates (for 6 h), with the exception of the Control group, the EC-LPS group, BV-LPS group and EC-BV combined group were respectively induced by the addition of EC-LPS (10  $\mu$ g/ml) alone, BV-LPS (60  $\mu$ g/ml) alone, or a combination of EC-LPS and BV-LPS. After 48 h induction, the medium was discarded, 1 ml 4% paraformaldehyde was added and fixed at room temperature for 30 min. At room temperature, 0.5% Triton X-100 (Beijing Solarbio Technology, Co., Ltd.) was added and allowed to permeate the cells for 20 min, followed by washing of the cells thrice, for 5 min each time, with phosphate-buffered normal saline (PBS; Beijing Solarbio Technology Co., Ltd.) and sealing with immunochromic sealing solution (Beyotime Institute of Biotechnology) for 60 min. The immunochromic sealing solution was subsequently removed and rabbit polyclonal antibodies against epithelial cadherin (E-cadherin; 1:200; cat. no. AF0131; Affinity Biosciences, Ltd.),  $\alpha$ -smooth muscle actin ( $\alpha$ -SMA; 1:200; cat. no. AF1032; Affinity Biosciences, Ltd.) and vimentin (1:200; cat. no. AF7013; Affinity Biosciences, Ltd.) were then added overnight at 4°C. The cells were subsequently washed five times (5 min each time) with cold PBS. FITC-labeled goat anti-rabbit IgG secondary antibody (1:200; cat. no. S0008; Affinity Biosciences, Ltd.) was incubated with the cells at room temperature and the cells were kept in the dark for 2 h. The nuclei were then stained with DAPI (Beyotime Institute of Biotechnology) for 5 min at room temperature, prior to removal of the DAPI staining solution and washing the cells three times with PBS. The cell slides were removed from the plate hole and the side containing the cells was then placed on a slide containing an anti-fluorescence quenching agent (cat. no. P0126; Beyotime Institute of Biotechnology). Finally, images were captured and analyzed using a fluorescence microscope (Olympus Corporation) and ImageJ software v1.49 (National Institutes of Health).

**RT-qPCR.** Lung tissues or A549 cells were treated with TriQuick Reagent total RNA extraction reagent (Beijing Solarbio Technology Co., Ltd.) and lung tissues were crushed by passing through a high-throughput tissue grinder (Ningbo Xinzhi Biotechnology Co., Ltd.) at 4°C. Subsequently, the RNA

was extracted according to the instructions provided in the kit. The first-strand cDNA was then synthesized using a HiFiScript gDNA Removal cDNA Synthesis Kit (Beijing ComWin Biotech Co., Ltd.) according to the instructions described by the manufacturer. RT-qPCR was performed with UltraSYBR Mixture (Beijing ComWin Biotech Co., Ltd.) and a CFX96 quantitative PCR instrument (Bio-Rad Laboratories, Inc.), according to the manufacturer's instructions. The qPCR was performed at 95°C for 10 min, followed by 40 cycles at 95°C for 15 sec and 60°C for 1 min. After having performed the amplification reaction, the average threshold cycle number was used as the Ct value of each sample. GAPDH was used as the reference gene for normalization of the mRNA levels and the relative expression levels of the target genes were calculated using the  $2^{-\Delta\Delta C_t}$  method (18). The RT-qPCR experiments were repeated for three times. Primer synthesis was carried out by Shanghai Shengong Bioengineering Co., Ltd. and the primer sequences for the human and mice genes are shown in Table I.

**Western blot analysis.** Total protein was extracted from lung tissue or A549 cells and the protein concentration was determined by following the instructions in the protein extraction kit (Beijing Solarbio Technology Co., Ltd.) and the BCA protein quantification kit (Beijing Solarbio Technology Co., Ltd.), respectively. According to the determined protein concentration, 1,000  $\mu$ g sample was diluted to 200  $\mu$ l with PBS solution and then 50  $\mu$ l 5X protein loading buffer (Beijing Solarbio Technology Co., Ltd.) was added, mixed and boiled in boiling water for 5 min, prior to storage at -20°C for later use. The samples (10  $\mu$ l/40  $\mu$ g) were then subjected to SDS-PAGE (8%) before being transferred on to a PVDF membrane and blocking with 5% skimmed milk powder for 2 h at room temperature. Subsequently, the protein samples were incubated with rabbit polyclonal antibodies against E-cadherin (1:1,000; cat. no. AF0131; Affinity Biosciences, Ltd.),  $\alpha$ -SMA (1:1,000; cat. no. AF1032; Affinity Biosciences, Ltd.), vimentin (1:1,000; cat. no. AF7013; Affinity Biosciences, Ltd.) and GAPDH (1:5,000; cat. no. AP0063; Biogot Technology, Co, Ltd) overnight at 4°C. The membranes were then washed 3 times with TBST (1X) containing 0.05% Tween20 (10 min each wash) and incubated with goat anti-rabbit IgG (H+L)-HRP secondary

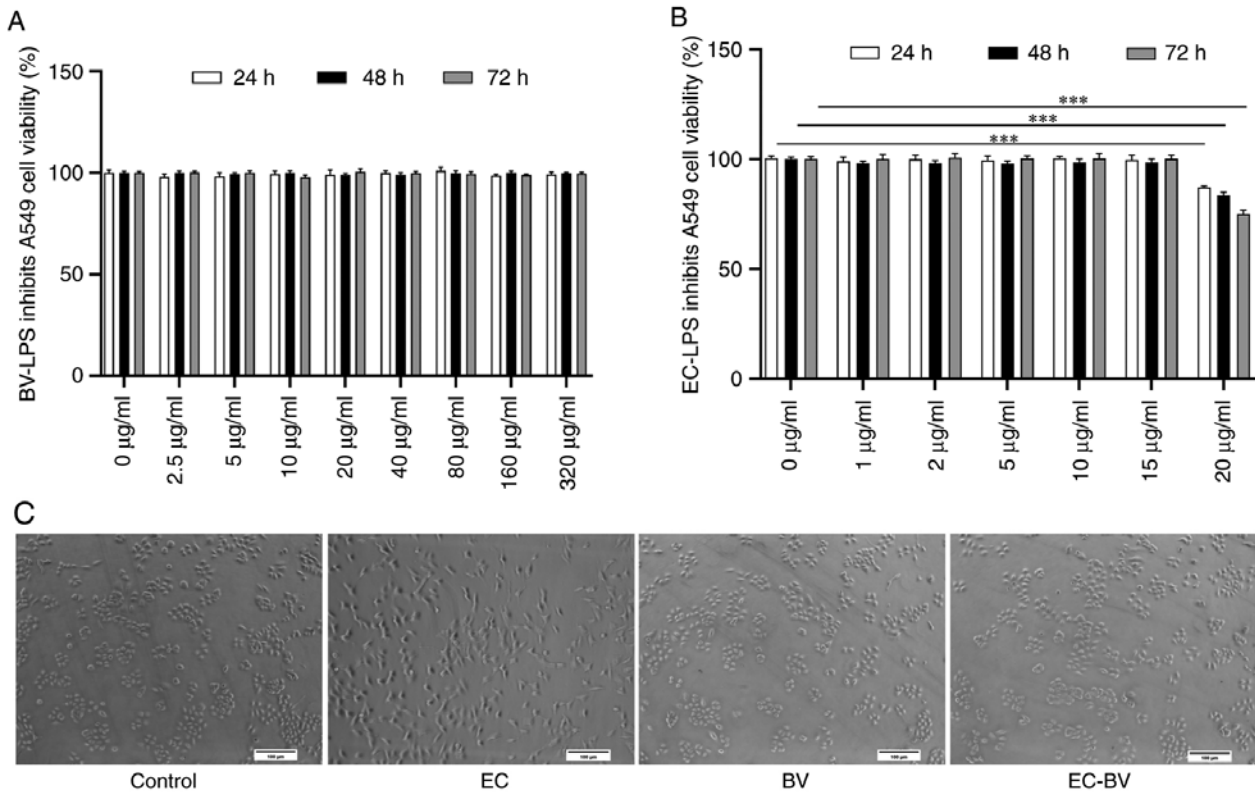


Figure 1. BV-LPS abolishes EC-LPS induced morphological changes in A549 cells. A549 cells were treated with (A) BV-LPS or (B) EC-LPS for 72 h and cell viability was analyzed using MTT assay. (C) BV-LPS abolished EC-LPS-induced morphological changes in A549 cells (magnification, x200). \*\*\* $P < 0.001$  vs. 0  $\mu\text{g/ml}$  group. BV-LPS, LPS extracted from *Bacteroides vulgatus*; EC-LPS, LPS extracted from *Escherichia coli*; Control, control group; EC, EC-LPS group; BV, BV-LPS group; EC-BV, co-treated with EC-LPS and BV-LPS group.

antibody (1:5,000; cat. no. BS13278; Biogot Technology, co, Ltd, USA) for 2 h at room temperature. Exposure development was performed using ECL chemiluminescent color developer (Biogot Technology, Co, Ltd.) and ChemicDoc XRS<sup>+</sup> imager (Bio-Rad Laboratories, Inc.). After scanning the exposed protein bands, ImageJ software v1.49 (National Institutes of Health) was used to calculate the optical density of the protein bands and the levels of the target proteins of interest were normalized against that of GAPDH as the control protein.

**Histological and immunohistochemical analysis.** Lung tissue fixed at room temperature for 48 h with 4% paraformaldehyde, followed by dehydration (slides washed in 100, 95, 80 and 75% alcohol for 2 min each), embedding and sectioning (5  $\mu\text{m}$ -thick sections). To observe the histomorphology of lung injury, hematoxylin and eosin (H&E) (cat. no. G1003; Wuhan Servicebio Technology Co., Ltd.) stained for 5 min at room temperature, following the manufacturer's protocol. The lung sections were also immunostained with rabbit polyclonal antibodies raised against IL-1 $\beta$  (cat. no. P420B; Thermo Fisher Scientific, Inc.), IL-6 (cat. no. GB11117; Wuhan Servicebio Technology Co., Ltd.), TNF- $\alpha$  (cat. no. GB11188; Wuhan Servicebio Technology Co., Ltd.), TLR4 (cat. no. GB11519; Wuhan Servicebio Technology Co., Ltd.), bone morphogenic protein and activin membrane-bound inhibitor (BAMBI) (cat. no. PA5-109443; Thermo Fisher Scientific, Inc.) and Snail (cat. no. GB11132; Wuhan Servicebio Technology Co., Ltd.) overnight at 4°C, all antibodies at a dilution of 1:100. Subsequently, the lung sections

were incubated at room temperature with biotinylated secondary antibodies (cat. no. GB23303; Wuhan Servicebio Technology Co., Ltd.) for 50 min, followed by staining with 3,3'-diaminobenzidine (DAB) solution (cat. no. G1212; Wuhan Servicebio Technology Co., Ltd.) to detect the avidin-biotin complex signal. Finally, images were captured and analyzed using a microscope (E100; Nikon Corporation) equipped with a digital camera and ImageJ software v1.49 (National Institutes of Health).

**Statistical analysis.** All data are shown as the mean  $\pm$  standard deviation and statistical analyses were performed using statistical software (SPSS version 26.0; IBM Corp.). Statistically significant differences among the results were analyzed by one-way analysis of variance (ANOVA) with Tukey's post hoc test.  $P < 0.05$  was considered to indicate a statistically significant difference.

## Results

**BV-LPS abolishes EC-LPS-induced morphological changes in A549 cells.** EC-LPS has been demonstrated to be an effective inducer of EMT in epithelial cells (16,19,20). In the present series of experiments, A549 cells were cultured in different concentrations of EC-LPS and BV-LPS for 72 h in order to determine the appropriate dose required for the EMT-induction model of EC-LPS and the appropriate dose for administration of BV-LPS. As shown in Fig. 1A and B, the results of MTT assay showed that 0-15  $\mu\text{g/ml}$  EC-LPS and 0-320  $\mu\text{g/ml}$  BV-LPS had no effect on the viability of A549

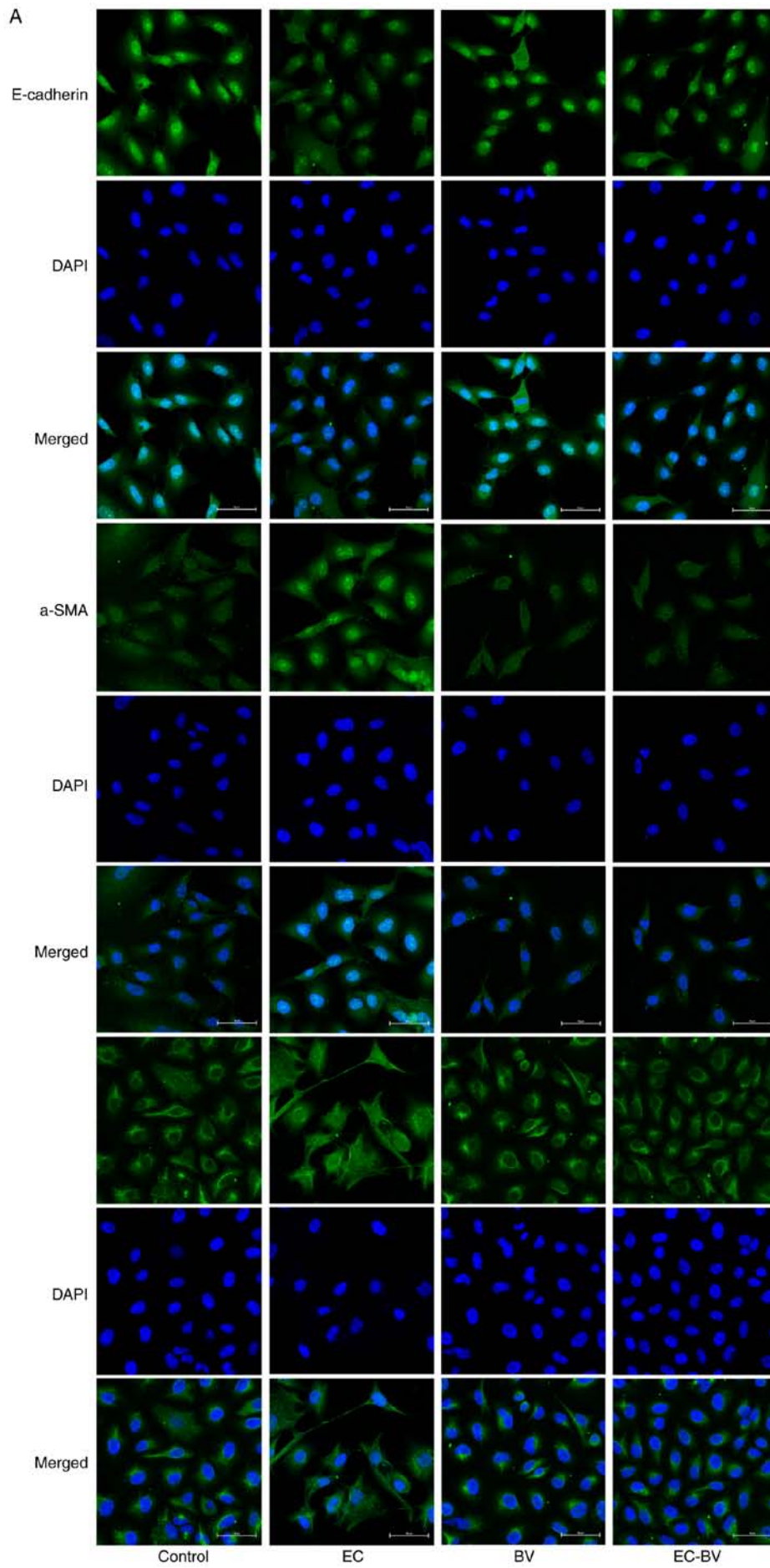


Figure 2. Continued.

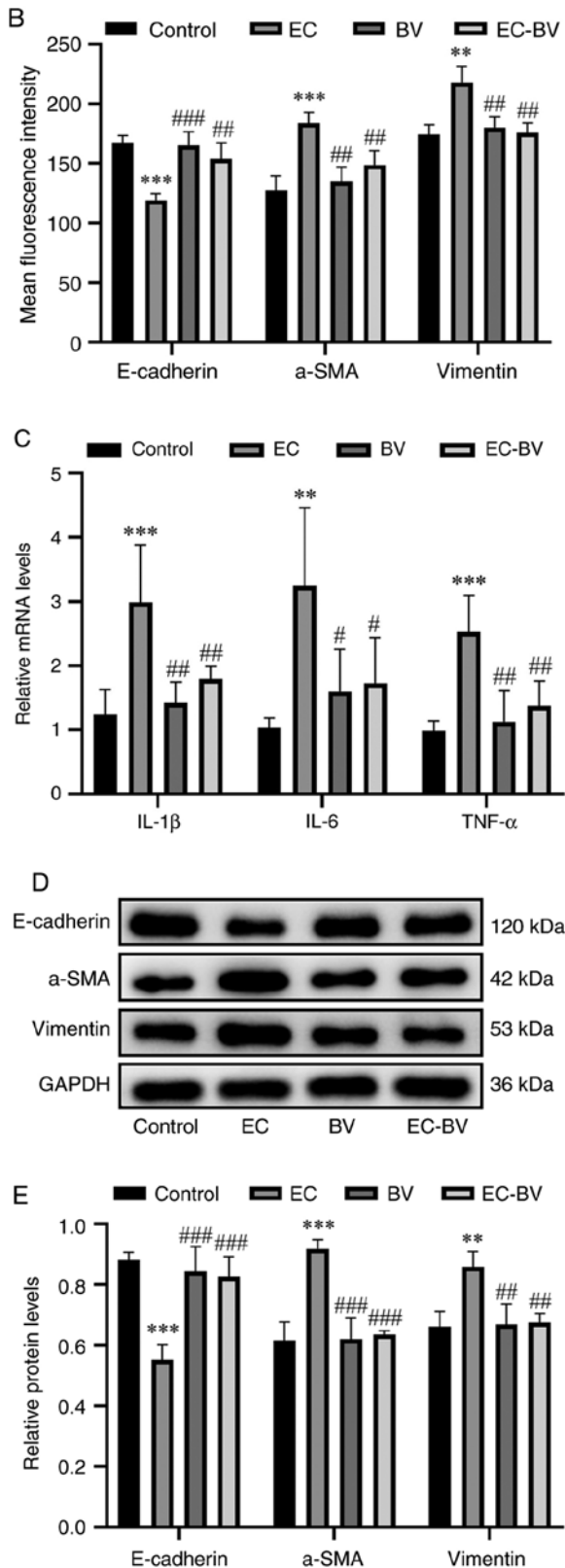


Figure 2. BV-LPS abolishes EC-LPS-induced inflammation and EMT in A549 cells. (A and B) Immunofluorescence staining showed that BV-LPS could abolish EC-LPS-induced EMT in A549 cells (magnification, x600). (C) Reverse transcription-quantitative PCR assay showed that BV-LPS could abolish EC-LPS-induced inflammation in A549 cells. (D and E) Western blot analysis showed that BV-LPS could abolish EC-LPS-induced EMT in A549 cells. \*\* $P < 0.01$  and \*\*\* $P < 0.001$  vs. the control group; # $P < 0.05$ , ## $P < 0.01$  and ### $P < 0.001$  vs. the EC-LPS group. BV-LPS, LPS extracted from *Bacteroides vulgatus*; EC-LPS, LPS extracted from *Escherichia coli*; EMT, epithelial-mesenchymal transition; Control, control group; EC, EC-LPS group; BV, BV-LPS group; EC-BV, co-treated with EC-LPS and BV-LPS group.

cells. However, it was also noted that incubation of A549 cells with 10  $\mu\text{g/ml}$  EC-LPS for 48 h resulted in a more stretched, or elongated, spindle-shaped morphology of the cells (Fig. 1C), which is a typical feature of EMT (21). However, this morphological change was effectively abolished by treatment with BV-LPS.

*BV-LPS abolishes EC-LPS-induced inflammation and EMT in A549 cells.* A549 cells were subsequently treated with EC-LPS (10  $\mu\text{g/ml}$ ) and BV-LPS (60  $\mu\text{g/ml}$ ) alone or in combination for up to 48 h. Immunofluorescence staining and western blot analysis revealed that, consistent with the morphological changes, EC-LPS treatment led to a significant upregulation of the mesenchymal marker proteins  $\alpha$ -SMA and vimentin, whereas the epithelial cell marker protein E-cadherin was markedly downregulated, although treatment with BV-LPS abolished these changes (Fig. 2A, B, D and E). In a subsequent series of experiments, the mRNA expression levels of the inflammatory cytokines IL-1 $\beta$ , IL-6 and TNF- $\alpha$  were also examined by RT-qPCR. As shown in Fig. 2C, EC-LPS treatment led to a significant upregulation of these inflammatory cytokines, whereas treatment with BV-LPS almost completely abolished the effects of EC-LPS. Taken together, these results suggested that BV-LPS was able to counteract the EC-LPS-induced inflammation and EMT observed in A549 cells.

*BV-LPS abolishes EC-LPS-induced lung injury and inflammation in vivo.* At 4 weeks following drug administration, the protective effect of BV-LPS was further examined in a mouse EMT model. The body weight and wet lung weight of mice were counted and there was no significant difference in body weight before administration. EC-LPS treatment resulted in a significant decrease in body weight and a significant increase in wet lung weight, while BV-LPS treatment abolished these changes (Fig. 3A-C). Using the percentage of lung wet weight/body weight as the lung index, the calculated results showed that BV-LPS treatment led to a canceling-out of the increase in lung index induced by EC-LPS in mice (Fig. 3D). The extent of lung injury was evaluated using H&E staining. As shown in Fig. 3E, EC-LPS induced a thickening of the alveolar wall and the collapse of alveoli, with an unclear structure of lung tissue in mice, although these changes were greatly ameliorated by treatment with BV-LPS. The mRNA and protein expression levels of the inflammatory cytokines (IL-1 $\beta$ , IL-6 and TNF $\alpha$ ) were also detected and a notable reduction in the release of IL-1 $\beta$ , IL-6 and TNF- $\alpha$  was observed following BV-LPS therapy (Fig. 3F and G). Collectively, these results suggested that BV-LPS could abolish EC-LPS-induced lung injury and inflammation in mice lung tissue.

*BV-LPS abolishes EC-LPS induced EMT in vivo.* In a subsequent set of experiments, western blotting and RT-qPCR were employed to detect the levels of mesenchymal marker proteins and epithelial marker proteins. The results were found to be consistent with those obtained with the A549 cell experiments; namely,  $\alpha$ -SMA and vimentin were significantly upregulated and E-cadherin was markedly downregulated, upon treatment with EC-LPS, whereas BV-LPS therapy led to the reversal of these changes (Fig. 4A-C). Taken together,

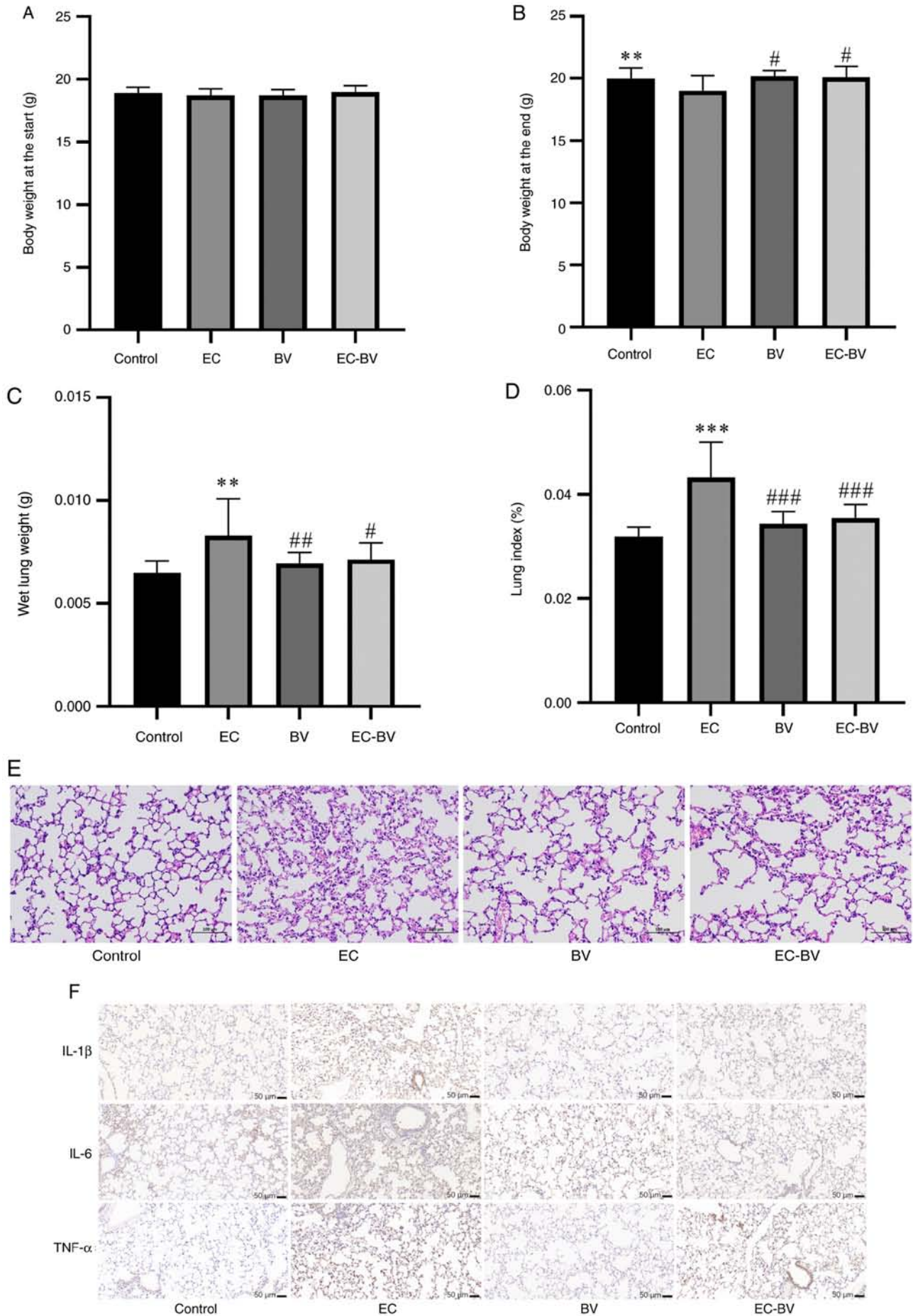


Figure 3. Continued.

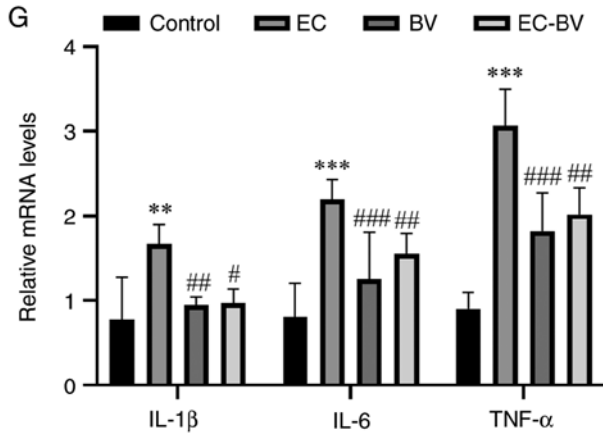


Figure 3. BV-LPS abolishes EC-LPS-induced lung injury and inflammation in mice. EC-LPS treatment resulted in (A and B) a significant decrease in body weight and (C) a significant increase in wet lung weight, while BV-LPS treatment abolished these changes. (D) BV-LPS was found to abolish the increase in the lung index induced by EC-LPS. (E) Hematoxylin and eosin staining of lung tissue, showing that BV-LPS could abolish EC-LPS-induced lung injury in mice (magnification,  $\times 200$ ). (F) Immunohistochemical (scale bar,  $50 \mu\text{m}$ ) and (G) reverse transcription-quantitative PCR, showing that BV-LPS could abolish EC-LPS-induced lung inflammation in mice. \*\* $P < 0.01$  and \*\*\* $P < 0.001$  vs. the control group; # $P < 0.05$ , ## $P < 0.01$  and ### $P < 0.001$  vs. the EC-LPS group. BV-LPS, LPS extracted from *Bacteroides vulgatus*; EC-LPS, LPS extracted from *Escherichia coli*; Control, control group; EC, EC-LPS group; BV, BV-LPS group; EC-BV, co-treated with EC-LPS and BV-LPS group.

these results suggested that BV-LPS was also able to abolish EC-LPS-induced EMT in mice lung tissue.

*The TLR4/BAMBI/Snail pathway may be involved in the mechanism governing how BV-LPS abolishes EC-LPS-induced EMT.* The TLR4/BAMBI/Snail pathway is involved in the direct induction of EMT (10). TLR4, a receptor for LPS, is one of the strongest inducers of inflammation (22). The pseudoreceptor BAMBI acts as a regulator between LPS/TLR4 signaling and TGF- $\beta$ -induced EMT and it also functions as a negative regulator of the TGF- $\beta$  signaling pathway (23). However, Snail proteins have been shown to induce EMT and are promoted by the TGF- $\beta$  signaling pathway (24). The results of the RT-qPCR and western blot analyses, with the goal of detecting the levels of TLR4, BAMBI and Snail, revealed that EC-LPS treatment caused a significant upregulation of TLR4 and Snail, whereas BAMBI was markedly downregulated. Notably, BV-LPS treatment was able to reverse these changes (Fig. 5A and B). Taken together, these results suggested that the TLR4/BAMBI/Snail pathway may be involved in the mechanism via which BV-LPS could abolish EC-LPS-induced EMT.

## Discussion

The immunoinhibitory structure of low-acylated lipid A is conserved in *Bacteroides* and there are many *Bacteroides* species that produce lipopolysaccharides in the intestinal flora, among which *B. ovatus*, *B. uniformis* and *B. vulgatus* are the most dominant (13). The BV-LPS is a pentacyclated A-LPS that has been shown to antagonize P-LPS-induced inflammation (25,26); therefore, BV-LPS was selected for the A-LPS in the present study.

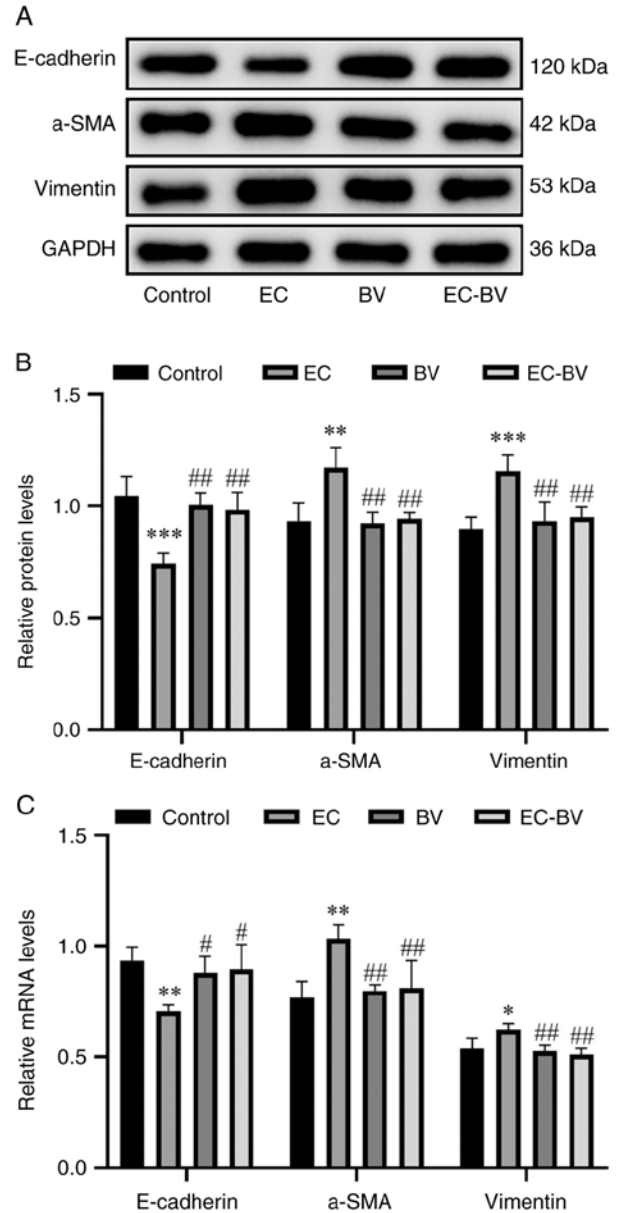


Figure 4. BV-LPS abolishes EC-LPS induced EMT in mice. (A and B) Western blot analysis, showing that BV-LPS could abolish EC-LPS-induced EMT in mice. (C) Reverse transcription-quantitative PCR also showed that BV-LPS could abolish EC-LPS-induced lung EMT in mice. \* $P < 0.05$ , \*\* $P < 0.01$  and \*\*\* $P < 0.001$  vs. the control group; # $P < 0.05$  and ## $P < 0.01$  vs. the EC-LPS group. BV-LPS, LPS extracted from *Bacteroides vulgatus*; EC-LPS, LPS extracted from *Escherichia coli*; EMT, epithelial-mesenchymal transition. Control, control group; EC, EC-LPS group; BV, BV-LPS group; EC-BV, co-treated with EC-LPS and BV-LPS group.

Previous studies have shown that EC-LPS, as an independent factor triggering EMT in epithelial cells (27), can be used to induce the EMT process in epithelial cells and lung tissues (16,19,20). Proteobacteria are a major contributor to P-LPS synthesis, whereas Bacteroidetes are a major contributor to A-LPS synthesis. It has been reported that *Bacteroides* contribute a mean of 79% of the total LPS in the intestinal flora of healthy subjects (13), so A-LPS is  $>4$  times higher than P-LPS in the intestinal flora of healthy subjects. Therefore, in the present study chose BV-LPS with a concentration 6 times higher than EC-LPS for the

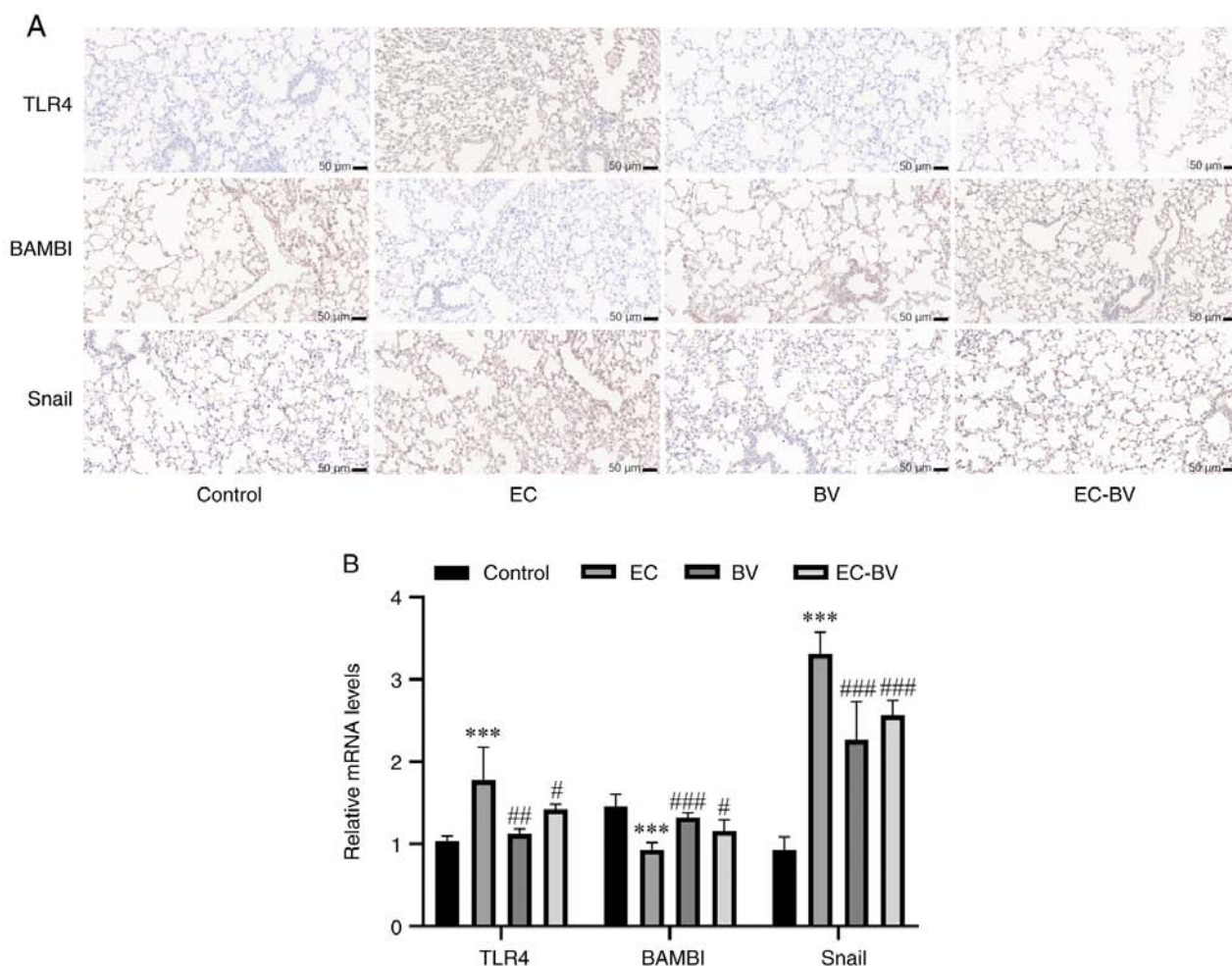


Figure 5. The TLR4/BAMBI/Snail pathway may be involved in BV-LPS abolished EC-LPS induced EMT. The (A) immunohistochemical and (B) reverse transcription-quantitative PCR showed that BV-LPS could reverse the downregulation of E-cadherin and upregulation of  $\alpha$ -SMA and vimentin induced by EC-LPS (scale bar, 50  $\mu$ m). \*\*\* $P$ <0.001 vs. the control group; # $P$ <0.05, ## $P$ <0.01 and ### $P$ <0.001 vs. the EC-LPS group. TLR4, Toll-like receptor 4; BAMBI, bone morphogenic protein and activin membrane-bound inhibitor; BV-LPS, LPS extracted from *Bacteroides vulgatus*; EC-LPS, LPS extracted from *Escherichia coli*; EMT, epithelial-mesenchymal transition;  $\alpha$ -SMA,  $\alpha$ -smooth muscle actin; Control, control group; EC, EC-LPS group; BV, BV-LPS group; EC-BV, co-treated with EC-LPS and BV-LPS group.

experiment. Inflammation is a key factor in pathological EMT (5) and EC-LPS-induced EMT models have been used both *in vivo* and *in vitro* (16,19,20). During EMT, the level of E-cadherin, a marker protein in epithelial cells, is decreased, while those of mesenchymal marker proteins, such as vimentin and  $\alpha$ -SMA, are increased (14,15). In the present study, it was found that the morphology of A549 alveolar epithelial cells exhibited clearly depolarized, mutual dispersion and fibrous growth under conditions of EC-LPS induction, whereas the treatment comprising a combination of BV-LPS with EC-LPS failed to induce the morphological changes of the A549 cells. The expression levels of the pro-inflammatory cytokines IL-1 $\beta$ , IL-6, TNF- $\alpha$  and the marker proteins vimentin and  $\alpha$ -SMA in mesenchymal cells were upregulated in A549 cells induced by EC-LPS, whereas the expression level of the marker protein E-cadherin in epithelial cells was downregulated. By contrast, treatment with BV-LPS combined with EC-LPS failed to induce these changes. Following EC-LPS induction, the lung index of mice was increased, the alveolar wall was found to have thickened, the alveolar

structure collapsed and the structure was unclear; moreover, the expression levels of the pro-inflammatory cytokines IL-1 $\beta$ , IL-6 and TNF- $\alpha$ , and the marker proteins vimentin and  $\alpha$ -SMA of mesenchymal cells, were upregulated, whereas the expression level of the marker protein E-cadherin in epithelial cells was downregulated. The addition of BV-LPS in combination with EC-LPS failed to induce these changes. The results of the *in vitro* cell experiments and *in vivo* experiments were therefore found to corroborate each other, both supporting that BV-LPS could effectively counteract EC-LPS-induced inflammation, thereby preventing pathological EMT induced by an inflammatory microenvironment.

The pseudoreceptor BAMBI is expressed in numerous organs, including lung tissue and is involved in the development of fibrosis and cancer in these organs (28-30). TLR4 is highly expressed in diseased skin and lung tissues and is associated with extracellular matrix remodeling and fiber formation (29). BAMBI is structurally homologous with TGF- $\beta$  receptor I (TGF- $\beta$  RI) and is a member of the TGF- $\beta$  type I receptor family, although it lacks an intracellular kinase domain and is

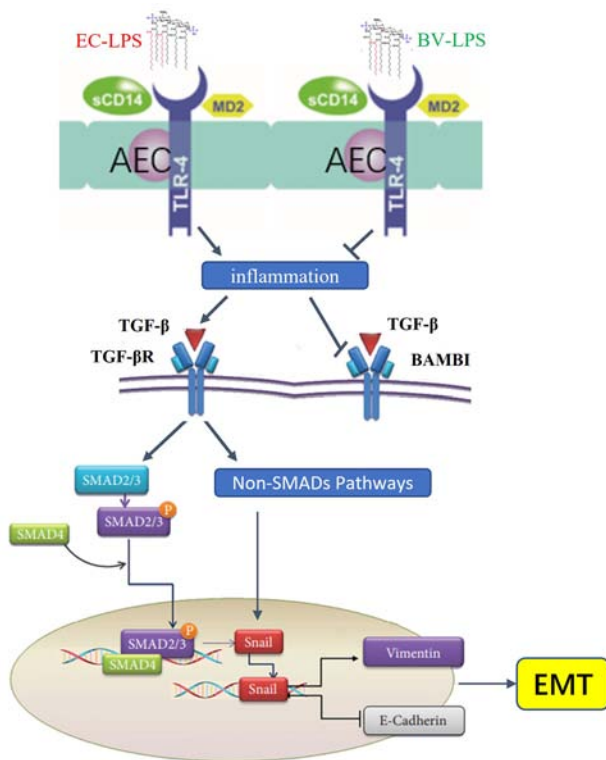


Figure 6. BV-LPS may antagonize EC-LPS-induced EMT via inhibiting the TLR4/BAMBI/Snail pathway. BV-LPS, LPS extracted from *Bacteroides vulgatus*; EC-LPS, LPS extracted from *Escherichia coli*; EMT, epithelial-mesenchymal transition; TLR4, Toll-like receptor 4; BAMBI, bone morphogenic protein and activin membrane-bound inhibitor.

a negative regulator of the TGF- $\beta$  signaling pathway (31,32). The LPS/TLR4 signaling pathway has been shown to reduce TGF- $\beta$  binding to BAMBI via inhibiting BAMBI expression, which has the effect of inducing the TGF- $\beta$  response to EMT, ultimately leading to progressive fiber formation (22,30). TGF- $\beta$  is able to trigger the EMT through both the SMAD and non-SMAD signaling pathways (33). In the SMAD pathway, EMT is activated by the TGF- $\beta$ 1/SMAD/Snail signaling axis, leading to the induction of EMT-dependent fibrosis (34-36). TGF- $\beta$  receptor consists of three receptor types, RI, RII and RIII (37). TGF- $\beta$  binds to RIII and is subsequently recruited to cell membrane RII/RI, which is phosphorylated to form an activated heterotetramer serine/threonine kinase complex (38). Phosphorylation activates the SMAD2/3 protein, leading to the subsequent formation of a phosphorylated SMAD2/3-SMAD4 complex with SMAD4 (39). The SMAD complex migrates to the nucleus and induces Snail via activating transcription factors (40,41). Snail induces the EMT process, thereby leading to the downregulation of epithelial markers such as E-cadherin and the upregulation of mesenchymal markers such as vimentin and  $\alpha$ -SMA (24,42). TGF- $\beta$ 1 has also been shown to induce EMT by activating Snail via the non-SMAD-dependent PI3K/AKT and MAPK/ERK1/2 signaling pathways (43). In the present study, the expression levels of TLR4 and BAMBI were significantly upregulated and BAMBI was significantly downregulated, in lung tissue induced by EC-LPS. However, these changes were reversed when the tissue sections were treated with a combination of BV-LPS and EC-LPS. Taken together, these results suggested that BV-LPS

may antagonize EC-LPS-induced EMT through inhibiting the TLR4/BAMBI/Snail pathway, as shown in Fig. 6.

However, the present study did have certain limitations. First, the concentration ratio of BV-LPS which competitively inhibits EC-LPS activity was not explored. Second, only preliminary observations have been made of the mechanism underlying how BV-LPS may prevent EC-LPS-induced EMT and further studies are required to fully elucidate the mechanism. Subsequent experiments will determine the concentration ratio of BV-LPS to competitively inhibit EC-LPS activity and identify the mechanism of BV-LPS preventing EMT induced by EC-LPS via the TLR4/BAMBI/Snail pathway with inhibitors or additional evidence when further funding is obtained. In conclusion, the present study demonstrated that BV-LPS can effectively prevent EC-LPS-induced EMT in mouse lung tissue and A549 cells and the underlying mechanism may be associated with inhibition of TLR4/BAMBI/Snail pathway.

### Acknowledgements

Not applicable.

### Funding

The present study was supported by the NHC Key Laboratory of Pulmonary Immune-related Diseases (grant no. 2019PT320003), the Guizhou Province Department of Education Youth Science and Technology Talent Growth Project [Guizhou Education KY word; grant no. (2022)266], the National Natural Science Foundation of China (grant no. 82260872) and the Program of Innovative Scientific and Technological Talent Team of Guizhou Province (grant no. 2020-5010).

### Availability of data and materials

The datasets used and/or analyzed during the current study are available from the corresponding author on reasonable request.

### Authors' contributions

HZ and CY designed the study. YL, MX, ZK, QX, JY and ZS performed the experiments. YL, WC, JO and HZ analyzed the data. YL and HZ drafted and revised the manuscript. YL and CY confirm the authenticity of all the raw data. All authors read and approved the final manuscript.

### Ethics approval and consent to participate

The animal study protocol was reviewed and approved by the Experimental Animal Ethics Committee of Guizhou University of Traditional Chinese Medicine (approval no. 20220039).

### Patient consent for publication

Not applicable.

### Competing interests

The authors declare that they have no competing interests.

## References

- Rout-Pitt N, Farrow N, Parsons D and Donnelley M: Epithelial mesenchymal transition (EMT): A universal process in lung diseases with implications for cystic fibrosis pathophysiology. *Respir Res* 19: 136, 2018.
- Yang Y, Hu L, Xia H, Chen L, Cui S, Wang Y, Zhou T, Xiong W, Song L, Li S, *et al*: Resolvin D1 attenuates mechanical stretch-induced pulmonary fibrosis via epithelial-mesenchymal transition. *Am J Physiol Lung Cell Mol Physiol* 316: L1013-L1024, 2019.
- Yang ZC, Qu ZH, Yi MJ, Shan YC, Ran N, Xu L and Liu XJ: MiR-448-5p inhibits TGF- $\beta$ 1-induced epithelial-mesenchymal transition and pulmonary fibrosis by targeting Six1 in asthma. *J Cell Physiol* 234: 8804-8814, 2019.
- Nieto MA, Huang RY, Jackson RA and Thiery JP: EMT: 2016. *Cell* 166: 21-45, 2016.
- López-Novoa JM and Nieto MA: Inflammation and EMT: An alliance towards organ fibrosis and cancer progression. *EMBO Mol Med* 1: 303-314, 2009.
- Fedele G, Nasso M, Spensieri F, Palazzo R, Frasca L, Watanabe M and Ausiello CM: Lipopolysaccharides from *Bordetella pertussis* and *Bordetella parapertussis* differently modulate human dendritic cell functions resulting in divergent prevalence of Th17-polarized responses. *J Immunol* 181: 208-216, 2008.
- Park BS, Song DH, Kim HM, Choi BS, Lee H and Lee JO: The structural basis of lipopolysaccharide recognition by the TLR4-MD-2 complex. *Nature* 458: 1191-1195, 2009.
- Lin TL, Shu CC, Chen YM, Lu JJ, Wu TS, Lai WF, Tzeng CM, Lai HC and Lu CC: Like Cures Like: Pharmacological activity of anti-inflammatory lipopolysaccharides from gut microbiome. *Front Pharmacol* 11: 554, 2020.
- Cardinelli CS, Sala PC, Alves CC, Torrinhas RS and Waitzberg DL: Influence of intestinal microbiota on body weight gain: A narrative review of the literature. *Obes Surg* 25: 346-353, 2015.
- Brown GC: The endotoxin hypothesis of neurodegeneration. *J Neuroinflammation* 16: 180, 2019.
- He Z, Zhu Y and Jiang H: Inhibiting toll-like receptor 4 signaling ameliorates pulmonary fibrosis during acute lung injury induced by lipopolysaccharide: An experimental study. *Respir Res* 10: 126, 2009.
- Hirschfeld M, Ma Y, Weis JH, Vogel SN and Weis JJ: Cutting edge: Repurification of lipopolysaccharide eliminates signaling through both human and murine toll-like receptor 2. *J Immunol* 165: 618-622, 2000.
- d'Hennezel E, Abubucker S, Murphy LO and Cullen TW: Total lipopolysaccharide from the human gut microbiome silences toll-like receptor signaling. *mSystems* 2: e00046-17, 2017.
- Ding Z, Wu X, Wang Y, Ji S, Zhang W, Kang J, Li J and Fei G: Melatonin prevents LPS-induced epithelial-mesenchymal transition in human alveolar epithelial cells via the GSK-3 $\beta$ /Nrf2 pathway. *Biomed Pharmacother* 132: 110827, 2020.
- Chen D, Qiu YB, Gao ZQ, Wu YX, Wan BB, Liu G, Chen JL, Zhou Q, Yu RQ and Pang QF: Sodium propionate attenuates the lipopolysaccharide-induced epithelial-mesenchymal transition via the PI3K/Akt/mTOR signaling pathway. *J Agric Food Chem* 68: 6554-6563, 2020.
- Zhang YQ, Liu YJ, Mao YF, Dong WW, Zhu XY and Jiang L: Resveratrol ameliorates lipopolysaccharide-induced epithelial mesenchymal transition and pulmonary fibrosis through suppression of oxidative stress and transforming growth factor- $\beta$ 1 signaling. *Clin Nutr* 34: 752-760, 2015.
- Tang S, Jiang X, Wu L, Chen S, Chen L, Jiang J, Yan P, Wang F, Tu K, Wang D, *et al*: Toll-like receptor 4 shRNA attenuates lipopolysaccharide-induced epithelial-mesenchymal transition of intrahepatic biliary epithelial cells in rats. *Biomed Pharmacother* 107: 1210-1217, 2018.
- Livak KJ and Schmittgen TD: Analysis of relative gene expression data using real-time quantitative PCR and the 2(-Delta Delta C(T)) method. *Methods* 25: 402-408, 2001.
- Liu W, Sun T and Wang Y: Integrin  $\alpha$  $\beta$ 6 mediates epithelial-mesenchymal transition in human bronchial epithelial cells induced by lipopolysaccharides of *Pseudomonas aeruginosa* via TGF- $\beta$ 1-Smad2/3 signaling pathway. *Folia Microbiol (Praga)* 65: 329-338, 2020.
- Gong JH, Cho IH, Shin D, Han SY, Park SH and Kang YH: Inhibition of airway epithelial-to-mesenchymal transition and fibrosis by kaempferol in endotoxin-induced epithelial cells and ovalbumin-sensitized mice. *Lab Invest* 94: 297-308, 2014.
- Li H, Li J, Zhang G, Da Q, Chen L, Yu S, Zhou Q, Weng Z, Xin Z, Shi L, *et al*: HMGB1-Induced p62 overexpression promotes snail-mediated epithelial-mesenchymal transition in glioblastoma cells via the degradation of GSK-3 $\beta$ . *Theranostics* 9: 1909-1922, 2019.
- Lim KH and Staudt LM: Toll-like receptor signaling. *Cold Spring Harb Perspect Biol* 5: a011247, 2013.
- He Y, Ou Z, Chen X, Zu X, Liu L, Li Y, Cao Z, Chen M, Chen Z, Chen H, *et al*: LPS/TLR4 signaling enhances TGF- $\beta$  response through downregulating BAMBI during prostatic hyperplasia. *Sci Rep* 6: 27051, 2016.
- Kaufhold S and Bonavida B: Central role of Snail1 in the regulation of EMT and resistance in cancer: A target for therapeutic intervention. *J Exp Clin Cancer Res* 33: 62, 2014.
- Yoshida N, Emoto T, Yamashita T, Watanabe H, Hayashi T, Tabata T, Hoshi N, Hatano N, Ozawa G, Sasaki N, *et al*: *Bacteroides vulgatus* and *Bacteroides dorei* Reduce gut microbial lipopolysaccharide production and inhibit atherosclerosis. *Circulation* 138: 2486-2498, 2018.
- Steimle A, Michaelis L, Di Lorenzo F, Kliem T, Münzner T, Maerz JK, Schäfer A, Lange A, Parusel R, Gronbach K, *et al*: Weak agonistic LPS restores intestinal immune homeostasis. *Mol Ther* 27: 1974-1991, 2019.
- Zhao L, Yang R, Cheng L, Wang M, Jiang Y and Wang S: LPS-induced epithelial-mesenchymal transition of intrahepatic biliary epithelial cells. *J Surg Res* 171: 819-825, 2011.
- Pulsikens WP, Rampanelli E, Teske GJ, Butter LM, Claessen N, Luirink IK, van der Poll T, Florquin S and Leemans JC: TLR4 promotes fibrosis but attenuates tubular damage in progressive renal injury. *J Am Soc Nephrol* 21: 1299-1308, 2010.
- Bhattacharyya S, Kelley K, Melichian DS, Tamaki Z, Fang F, Su Y, Feng G, Pope RM, Budinger GR, Mutlu GM, *et al*: Toll-like receptor 4 signaling augments transforming growth factor- $\beta$  responses: A novel mechanism for maintaining and amplifying fibrosis in scleroderma. *Am J Pathol* 182: 192-205, 2013.
- Seki E, De Minicis S, Osterreicher CH, Kluwe J, Osawa Y, Brenner DA and Schwabe RF: TLR4 enhances TGF- $\beta$ 2 signaling and hepatic fibrosis. *Nat Med* 13: 1324-1332, 2007.
- Lutz M and Knaus P: Integration of the TGF-beta pathway into the cellular signalling network. *Cell Signal* 14: 977-988, 2002.
- Chen J, Bush JO, Ovitt CE, Lan Y and Jiang R: The TGF-beta pseudoreceptor gene Bambi is dispensable for mouse embryonic development and postnatal survival. *Genesis* 45: 482-486, 2007.
- Zhang YE: Non-Smad pathways in TGF-beta signaling. *Cell Res* 19: 128-139, 2009.
- Sisto M, Lorusso L, Ingravallo G, Ribatti D and Lisi S: TGF $\beta$ 1-Smad canonical and -Erk noncanonical pathways participate in interleukin-17-induced epithelial-mesenchymal transition in Sjögren's syndrome. *Lab Invest* 100: 824-836, 2020.
- Fabregat I, Moreno-Cáceres J, Sánchez A, Dooley S, Dewidar B, Giannelli G and Ten Dijke P: IT-LIVER Consortium: TGF- $\beta$  signalling and liver disease. *FEBS J* 283: 2219-2232, 2016.
- Willis BC and Borok Z: TGF-beta-induced EMT: Mechanisms and implications for fibrotic lung disease. *Am J Physiol Lung Cell Mol Physiol* 293: L525-L534, 2007.
- Prud'homme GJ: Pathobiology of transforming growth factor beta in cancer, fibrosis and immunologic disease and therapeutic considerations. *Lab Invest* 87: 1077-1091, 2007.
- Heldin CH and Moustakas A: Signaling receptors for TGF- $\beta$  family members. *Cold Spring Harb Perspect Biol* 8: a022053, 2016.
- Wrighton KH, Lin X and Feng XH: Phospho-control of TGF-beta superfamily signaling. *Cell Res* 19: 8-20, 2009.
- Hill CS: Transcriptional control by the SMADs. *Cold Spring Harb Perspect Biol* 8: a022079, 2016.
- Brandl M, Seidler B, Haller F, Adamski J, Schmid RM, Saur D and Schneider G: IKK( $\alpha$ ) controls canonical TGF( $\beta$ )-SMAD signaling to regulate genes expressing SNAIL and SLUG during EMT in panc1 cells. *J Cell Sci* 123(Pt 24): 4231-4239, 2010.
- Sisto M, Lorusso L, Ingravallo G, Tamma R, Ribatti D and Lisi S: The TGF-1 signaling pathway as an attractive target in the fibrosis pathogenesis of Sjögren's Syndrome. *Mediators Inflamm* 2018: 1965935, 2018.
- Chen XF, Zhang HJ, Wang HB, Zhu J, Zhou WY, Zhang H, Zhao MC, Su JM, Gao W, Zhang L, *et al*: Transforming growth factor- $\beta$ 1 induces epithelial-to-mesenchymal transition in human lung cancer cells via PI3K/Akt and MEK/Erk1/2 signaling pathways. *Mol Biol Rep* 39: 3549-3556, 2012.

